Inorganic Chemistry

ARTICLE

pubs.acs.org/IC

Coordination-Driven Inversion of Handedness in Ligand-Modified PNA

Silvia Bezer,[†] Srinivas Rapireddy,[†] Yury A. Skorik,[‡] Danith H. Ly,[†] and Catalina Achim*[,†]

[†]Department of Chemistry, Carnegie Mellon University, 4400 Fifth Avenue, Pittsburgh, Pennsylvania, 15213-3890 United States

[‡]Department of Pharmaceutical Engineering, St. Petersburg State Chemical Pharmaceutical Academy, 14 Prof. Popov Street, St. Petersburg, 197022 Russian Federation

Supporting Information

ABSTRACT:

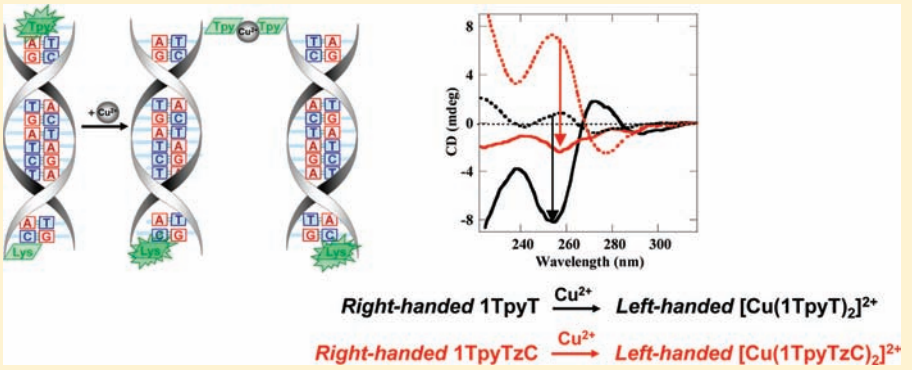

Peptide nucleic acid (PNA) is a synthetic analogue of DNA, which has the same nucleobases as DNA but typically has a backbone based on aminoethyl glycine (Aeg). PNA forms duplexes by Watson Crick hybridization. The Aeg-based PNA duplexes adopt a chiral helical structure but do not have a preferred handedness because they do not contain a chiral center. An L-lysine situated at the C-end of one or both strands of a PNA duplex causes the duplex to preferably adopt a left-handed structure. We have introduced into the PNA duplexes both a C-terminal L-lysine and one or two PNA monomers that have a γ-(*S*)-methyl-aminoethyl glycine backbone, which is known to induce a preference for a right-handed structure. Indeed, we found that in these duplexes the γ-methyl monomer exerts the dominant chiral induction effect causing the duplexes to adopt a right-handed structure. The chiral PNA monomer had a 2,2′:6′,2″-terpyridine (*Tpy*) ligand instead of a nucleobase and PNA duplexes that contained one or two *Tpy*s formed $[Cu(Tpy)_2]^{2+}$ complexes in the presence of Cu^{2+}. The CD spectroscopy studies showed that these metal-coordinated duplexes were right-handed due to the chiral induction effect exerted by the *S-Tpy* PNA monomer(s) except for the cases when the $[Cu(Tpy)_2]^{2+}$ complex was formed with *Tpy* ligands from two different PNA duplexes. In the latter case, the metal complex bridged the two PNA duplexes and the duplexes were left-handed. The results of this study show that the preferred handedness of a ligand-modified PNA can be switched as a consequence of metal coordination to the ligand. This finding could be used as a tool in the design of functional nucleic-acid based nanostructures.

INTRODUCTION

The unique double helix structure of DNA has been the inspiration for the biomimetic synthesis of numerous helical structures, including molecules comprising polytopic ligands coordinated to transition metal ions. In recent years, numerous nucleic acid duplexes that contained one or more transition metal complexes functioning as metal-based, alternative base pairs have been synthesized. These duplexes have been based mostly on DNA,[1] but also on pseudopeptide nucleic acid (PNA), locked nucleic acid (LNA), or glycol nucleic acid (GNA).[2] PNA has the same nucleobases as DNA but has a pseudopeptide backbone that is commonly based on the aminoethyl glycine (Aeg) scaffold, and thus is charge neutral (Scheme 1). The charge-neutral character of the PNA backbone makes it unique when it comes to the incorporation of metal complexes in PNA as alternative base pairs because the overall charge of the inorganic—PNA ensemble can be determined exclusively by the inorganic component of the ensemble.

PNA can form homo PNA·PNA duplexes that have a chiral, helical structure resembling that of DNA but with a smaller twist and, consequently, a larger number of base pairs per turn than B-DNA.[3] The aminoethyl glycine does not contain a chiral center and, consequently, the Aeg-based PNA duplexes do not have an intrinsic preferred handedness but they can adopt one if a chiral moiety is introduced into the PNA. Chiral amino acids such as L- or D-Lys situated at the C-terminus of the PNA strands have been shown to exert a chiral induction effect that leads to enantiomeric

Received: April 23, 2011
Published: November 07, 2011

Scheme 1. Chemical Structure of PNA and γ-PNA Monomers (B Represents a G, C, A, or T Nucleobase)

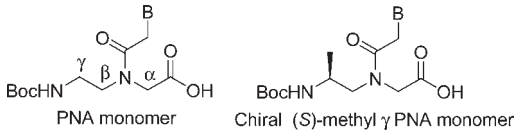

excess in solutions of homo-PNA duplexes.[3c,d,4] This effect measured by CD spectroscopy in solution is not strong enough to persist in crystals of PNA duplexes that had a terminal L-amino acid, which to date all contained a 1:1 mixture of left-handed and right-handed duplexes.[3c−e] Recent studies by Green and collaborators have led to the conclusion that (1) the PNA·PNA duplexes exist in solution as a dynamic ensemble of conformational states that depends on the nature of the terminal amino acid and on the sequence and length of the duplexes, and (2) the terminal amino acid interacts directly with the adjacent nucleobases and it exerts not only a chiral effect but a general structural effect on the duplex that extends beyond the nucleobases proximal to the amino acid.[4c] In our previous studies of the structure of a palindromic 8-base pair PNA duplex, we have identified hydrogen bonds between the backbone and side-chain of the C-terminal L-lysine of the duplex on one hand and the backbone or nucleobases close to the end of neighboring PNA duplexes on the other hand that may be similar to the ones by which the L-lysine exerts its chiral induction effect in solution.[3e]

A preferred handedness can also be induced in PNA duplexes by a stereogenic center at the α-[5] or γ-[6]position (Scheme 1). Recently, some of us have shown that in particular the incorporation of an (*S*)-Me stereogenic center at the γ-backbone position induced the formation of a right-handed structure even in a single-stranded (ss) PNA.[6b]

Most of the transition complexes that have been incorporated in DNA or PNA have four (almost) coplanar donor atoms from aromatic ligands, a design in which the steric interactions between the duplex and complex are small and π stacking is possible between the aromatic ligands in the metal complex and the adjacent nucleobase pairs. The metal binding sites designed for DNA included either two bidentate ligands or a pair of tridentate and monodentate ligands, which formed [2 + 2] or [3 + 1] complexes, respectively. Some of the metal ions in these complexes can coordinate two more ligands from the solvent or adjacent nucleobases, which do not contribute directly to the duplex stability but can affect it indirectly through steric interactions.[7] This biomimetic strategy led to supramolecular structures that contain transition metal ions at predefined positions.[2,8] We have applied this strategy to PNA, wherein we replaced an A:T base pair situated in the center of a ten base pair PNA duplex (**PNA** in Chart 1) with a pair of 8-hydroxyquinoline or 2,2′-bipyridine ligands to create [2 + 2] metal binding sites in the duplex.[9] Transition metal ions coordinated to the ligands in the modified PNA duplexes. The resulting metal-containing PNA duplexes were usually more stable than the corresponding metal-free, ligand-modified duplexes. Müller et al. suggested the potential use of the tridentate 2,2′:6′,2″-terpyridine (*Tpy*) together with a monodentate, nitrogen-coordinating ligand to create in nucleic acid duplexes an alternative, metal-mediated base pair of [3 + 1] type.[10] Switzer and collaborators have introduced in DNA duplexes a pair of a monodentate pyridine ligand (*Py*) and a tridentate ligand (3-*L*), which is geometrically

Chart 1. PNA Sequences

PNA	X_A	H_2N-Lys-CATCTAGTGA-H
	X_B	H-GTAGATCACT-Lys-NH_2
1TpyT	X_A.	NH_2-Lys-CATCTAGTGA-H
	S1.	H-GTAGATCACT*Tpy*-NH_2
1TpyXC	S4.	NH_2-Lys-CATC*Py*AGTGA-H
X = Py	S3.	H-GTAG*Tpy*TCACT-Lys-NH_2
X = Tz	S5.	NH_2-Lys-CATC*Tz*AGTGA-H
	S3.	H-GTAG*Tpy*TCACT-Lys-NH_2
2TpyY	S2.	NH_2-Lys-CATC*Tpy*AGTGA-H
Y = C	S3.	H-GTAG*Tpy*TCACT-Lys-NH_2
Y = T	S6.	NH_2-Lys-CATCTAGTGA*Tpy*-H
	S1.	H-GTAGATCACT*Tpy*-NH_2

similar to terpyridine. Based on the observation of a higher melting temperature of the ligand-modified DNA duplex in the presence of Ag^+ than in the absence of Ag^+, the authors concluded that a [3 + 1] complex $[(Py)Ag(3\text{-}L)]^+$ is formed within the DNA duplex.[11]

Metal coordination was also used to assemble nucleic acid duplexes with terminal ligands into nanostructures of various topologies.[12] For example, Fe^{2+} coordination to DNA duplexes that had terminal *Tpy* ligands led to the formation of DNA triangles in which $[Fe(Tpy)_2]^{2+}$ complexes connected the DNA duplexes to each other and acted as alternative Holliday junctions.[12a] The formation of $[Fe(Tpy)_2]^{2+}$ complexes has been used also for the allosteric control of oligonucleotide hybridization by metal-induced cyclization.[12b]

In this study we evaluated (1) the possibility of creating interduplex $[Cu(Tpy)_2]^{2+}$ complexes that bridge ss or dsPNA; (2) the possibility of creating Cu^{2+} complexes with [3 + 1] coordination of terpyridine−pyridine or terpyridine−tetrazole pairs of ligands that act as alternative base pairs in PNA duplexes; and (3) the modulation of the chiral induction effect exerted by an (*S*)-stereogenic center introduced in the backbone of a *Tpy*-PNA monomer by the coordination of Cu^{2+} to the *Tpy*. Our study shows that the large stability constant of the [3 + 3] $[Cu(Tpy)_2]^{2+}$ complexes favors the formation of these complexes over that of [3 + 1] complexes in PNA, that the chiral *S*-*Tpy* PNA monomer exerts a strong chiral effect on PNA, and that this effect can be turned off by metal coordination to the *Tpy* monomer.

EXPERIMENTAL SECTION

Materials. Acetaldehyde was treated with $NaHCO_3$ and distilled from $CaSO_4$. Tetrahydrofuran (THF) was distilled over Na and benzophenone. Dimethylformamide (DMF), diisopropylethylamine, and triethylamine were distilled from CaH_2 and stored over molecular sieves. Dry CH_2Cl_2 was distilled from CaH_2 prior to use. Acetylpyridine and 2,2,6,6-tetramethylpiperidine were distilled from $CaSO_4$. All other reagents were obtained from commercially available sources, as analytical grade, and were used without further purification. All reactions were monitored by TLC on SiO_2 (UV detection).

The *tert*-butyl 2-(2-(*tert*-butoxycarbonyl)ethylamino)acetate and ethyl 2-(2-(*tert*-butoxycarbonyl)-(*S*)-propylamino)acetate were prepared according to published procedures.[13] The 2-(pyridin-4-yl)acetic acid and 2-(1H-tetrazol-1-yl)acetic acid are commercially available.

dx.doi.org/10.1021/ic200855p |*Inorg. Chem.* 2011, 50, 11929–11937

Scheme 2. Ligand-Modified PNA Monomers

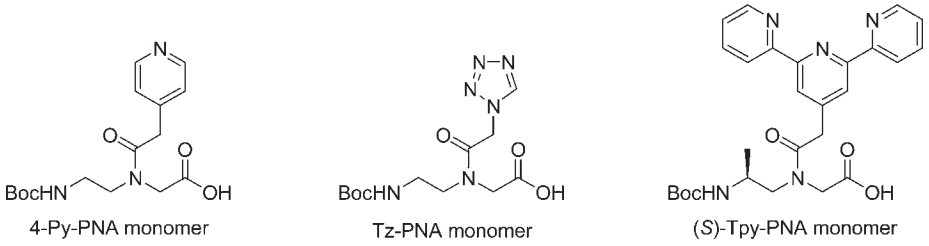

Table 1. Molecular Weight of PNA Oligomers

name	PNA sequence	calcd *m/z*	exptl *m/z*
X_A	NH_2-Lys-CATCTAGTGA-H	2855	2855
S1	NH_2-*Tpy*-TCACTAGATG-H	3114	3115
S2	NH_2-Lys-CATC-*Tpy*-AGTGA-H	2976	2977
S3	NH_2-Lys-TCACT-*Tpy*-GATG-H	2967	2967
S4	NH_2-Lys-CATC-*Py*-AGTGA-H	2808	2808
S5	NH_2-Lys-CATC-*Tz*-AGTGA-H	2799	2797
S6	NH_2-Lys-CATCTAGTGA-*Tpy*-H	3242	3242

The 2-(2,6-di(pyridin-2-yl)pyridin-4-yl) acetic acid and coupling of the acetic acid derivatives of all ligands to the PNA backbone was done according to literature procedures (Schemes 2 and S1 and S2 in the Supporting Information).[14]

^{1}H NMR spectra have been recorded on a Bruker Cryospec WM 300. A Finnegan Mattson instrument was used for electrospray mass spectrometry (ES-MS).

Solid-Phase PNA Synthesis. PNA oligomers were prepared by solid-phase peptide synthesis using the Boc-protection strategy (Table 1).[15] PNA monomers were purchased from Applied Biosystems and used without further purification. After cleavage from the solid support, PNA was precipitated using ethyl ether and purified by reversed-phase HPLC using a C18 silica column on a Waters 600 controller and pump. Absorbance was measured with a Waters 2996 photodiode array detector. Characterization of the oligomers was performed by MALDI-TOF mass spectrometry on an Applied Biosystems Voyager biospectrometry workstation with delayed extraction and an α-cyano-4-hydroxycinnamic acid matrix (10 mg/mL in 1:1 water/acetonitrile, 0.1%TFA).

CD Spectroscopy. CD spectra were measured for 5 μM dsPNA solutions in 10 mM sodium phosphate buffer (pH 7.0) on a JASCO J-715 spectropolarimeter equipped with a thermoelectrically controlled, single-cell holder. CD spectra were collected at 20 °C, using 1 nm bandwidth, 1 s response time, 100 nm/min speed, 20 mdeg sensitivity, and 12 scan accumulation.

UV−vis Spectroscopy. UV−vis experiments were performed on a Varian Cary 3 spectrophotometer equipped with a programmable temperature block, in quartz cells with 10-mm optical path. PNA stock solutions were prepared in deionized water at 95 °C, and the PNA concentrations were determined by UV−vis spectrophotometry, assuming ε(260 nm) = 8600, 6600, 13 700, and 11 700 cm^{-1} M^{-1} for the T, C, A, and G monomer, respectively,[16] and ε(260 nm) = 9750 and 2728 cm^{-1} M^{-1} for the *Tpy* and *Py* PNA monomers, respectively.[17] PNA solutions for melting curves and titration had concentrations in the micromolar range (5−50) and were prepared in the same sodium phosphate buffer. UV melting curves were recorded in the temperature range 5−95 °C for both cooling and heating modes, at the rate of 1 °C/min. The melting curves have been measured at the maximum absorbance of PNA, which was 267 nm. T_m is the inflection point of a sigmoidal function used to fit the melting curve.

UV−vis titrations were carried out by addition of standard 0.500 mM $Cu(NO_3)_2$ aqueous solution to PNA solutions in 10 mM sodium phosphate buffer at pH 7.0. The absorbance A was corrected (A_{corr}) for dilution and for the contribution of $Cu(NO_3)_2$ and PNA. All spectrophotometric titration curves were fitted with the HYPERQUAD 2000 program.[18]

RESULTS

Three new Boc-protected PNA monomers that had a terpyridine, pyridine, or tetrazole ligand instead of a nucleobase have been synthesized by coupling the acetic acid derivative of each ligand to the Boc-protected ester of aminoethyl glycine or methyl-aminoethyl glycine, followed by hydrolysis of the resulting ester with sodium hydroxide (Scheme 3).[6b,16] These PNA monomers were incorporated into PNA oligomers containing several nucleobases by solid-phase peptide synthesis using Boc-protection strategy.[15] The synthesis of Fmoc-protected PNA monomers containing pyridine[19] and terpyridine[20] has been previously reported. These Fmoc monomers have been used to synthesize supramolecular inorganic structures without nucleobases.[19−21]

PNA Sequences. The antiparallel, "non-modified" double-stranded (ds) PNA shown in Chart 1 (**PNA**) has been investigated extensively since the initial report of PNA in 1991.[22] We had synthesized five ligand-containing, ds PNAs whose sequences are related to that of the nonmodified ds **PNA** (Chart 1). In these duplexes, one (duplexes **1TpyT**, **1TpyPyC**, and **1TpyTzC**) or two *Tpy* ligands (duplexes **2TpyC** and **2TpyT**) were situated either at the terminus (duplexes **1TpyT** and **2TpyT**) or in the center (duplexes **2TpyC**, **1TpyTzC**, and **1TpyPyC**) of the duplex. The duplex **1TpyT** contained one terminal *Tpy* unit; consequently, it could form only an interduplex $[Cu(Tpy)_2]^{2+}$ complex and not an intraduplex complex. Duplexes **1TpyPyC** and **1TpyTzC** contained in the central position of the duplex a pair of *Tpy* and pyridine or tetrazole ligands, respectively, to create a [3 + 1] metal coordination site. The duplexes **2TpyPyC** and **2TpyPyT** contained a pair of *Tpy*s to create a [3 + 3] coordination site.

Variable-Temperature UV−vis Spectroscopy. The melting temperature of the nonmodified **PNA** is not affected by 1 equiv of Cu^{2+} (Figure 1a).[9] Duplex **1TpyT**, which has one terminal *Tpy*, showed cooperative binding with a melting temperature (T_m) comparable to that of the nonmodified **PNA**, which is 66 °C, but with higher hyperchromicity change (Figures 1 and S1, Table 2). This effect exerted by the terminal *Tpy* is similar to that previously observed for overhang nucleobases in nucleic acid duplexes.[23] The melting curve of **1TpyT** remained unchanged when measured in the presence of 0.5 equiv of Cu^{2+} per duplex (Figures 1b and S1, Table 2). A solution of the duplex **2TpyT**,

Scheme 3. 1. (a) DCC, DhbtOH, DMF; (b) EDC, DIPEA, DCM, r.t.; 2. (c) NaOH (25 M), EtOH; (d) NaOH (1 M), THF, 0°C

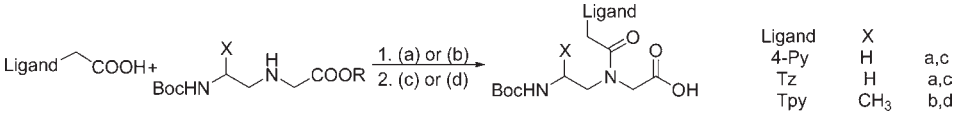

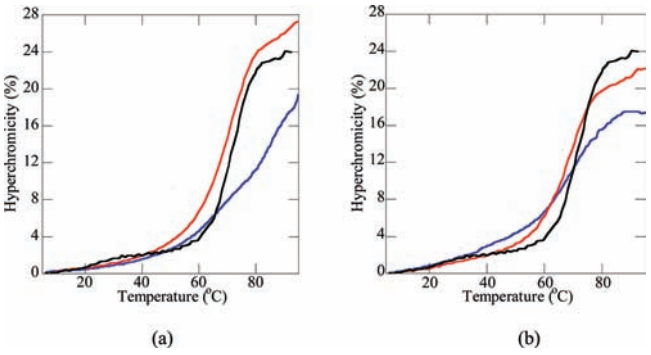

Figure 1. Melting curves of **1TpyT** (red) and **2TpyT** (blue) in the absence (a) and presence (b) of 0.5 equiv Cu^{2+}/Tpy. Solutions are 5 μM dsPNA in 10 mM sodium phosphate buffer at pH 7.0. For comparison purposes, the melting curve of the nonmodified **PNA** in the absence of Cu^{2+} is also shown (black).

which has two *Tpy* ligands at the same end, showed an increase in absorbance at 260 nm with increasing temperature suggestive of the formation of a duplex even more stable than **1TpyT** but a T_m could not be determined from this curve (Figures 1a and S1, Table 2). In the presence of 1 equiv of Cu^{2+} per duplex, **2TpyT** showed a cooperative transition typical for a PNA duplex, with a T_m of 70 °C (Figures 1b and S1, Table 2). In the absence of transition metal ions, duplexes **2TpyC**, which has a [3 + 3] pair of *Tpy-Tpy* ligands, and **1TpyXC** (where X = Py or Tz), which have a central [3 + 1] pair of *Tpy*−*Py* and *Tpy*−*Tz* ligands, have a T_m lower by ∼15 °C than the corresponding nonmodified **PNA** (Figure 2a and S1). This destabilization effect by a central pair of ligands that cannot form hydrogen bonds was previously observed in both PNA and DNA duplexes.[2] Duplexes **2TpyC** and **1TpyXC** showed in the presence of Cu^{2+} cooperative melting curves similar to each other and with a melting temperature of 45 °C (Figure 2b and S1).

UV−vis Titrations. Titration of a solution of the free ligand *Tpy* in pH 7.0 10 mM sodium phosphate buffer with Cu^{2+} caused a decrease in the absorbance at 250−300 nm and the appearance of two bands at 320−340 nm (Figure 3). For Cu^{2+} concentrations up to a Cu^{2+}/Tpy ratio of 1:2, an isosbestic point was observed at 309 nm and the titration curves at both 286 and 340 nm showed a linear increase with the concentration of Cu^{2+} (Figure 3 and Table 2). These spectroscopic features indicate the formation of a $[Cu(Tpy)_2]^{2+}$ complex. The addition of excess metal led to further but smaller changes in the UV spectra indicative of the conversion of $[Cu(Tpy)_2]^{2+}$ to $[Cu(Tpy)]^{2+}$. The same behavior was observed by Dobrawa et al. for titrations of *Tpy* dissolved in acetonitrile with Cu^{2+}, and was attributed to the sequential formation of $[Cu(Tpy)_2]^{2+}$ and $[Cu(Tpy)]^{2+}$, with one of the *Tpy* ligands in $[Cu(Tpy)_2]^{2+}$ being bidentate.[24]

The dominant feature of the UV spectra of both ss and ds *Tpy*-modified PNA was an absorbance band at 260 nm, which is primarily due to the $\pi-\pi^*$ transitions of the nucleobases. Smaller intensity bands were observed at 300−350 nm due to the *Tpy* ligand. These bands shifted bathochromically in the presence of Cu^{2+} (Figures 4−6 and S2−S4).

Given the sequence of the ss PNA **S3** and of the ds PNA **1TpyT**, $[Cu(Tpy)_2]^{2+}$ complexes formed by these PNAs with Cu^{2+} could be exclusively intermolecular, i.e., bridging two ss **S3** or two **1TpyT** PNAs. UV spectra of **S3** in the presence of increasing amounts of Cu^{2+} up to a Cu^{2+}/**S3** ratio of 1:2 showed an isosbestic point at 316 nm (Figure S2a). The titration curves at 305 and 340 nm showed an inflection point at Cu^{2+}/**S3** ratio of 1:2 (Figure S2b). The UV spectra of **1TpyT** in the presence of Cu^{2+} up to a 1:2 Cu^{2+}/Tpy ratio also show an isosbestic point at 315 nm (black curves in Figure 4a); changes in absorption take place at this wavelength for higher Cu^{2+} concentrations and another isosbestic point is observed at 340 nm (red spectra in Figure 4a). These observations are indicative of the stepwise formation of $[Cu(Tpy)_2]^{2+}$ and $[Cu(Tpy)]^{2+}$ complexes in the titration of **1TpyT** with Cu^{2+}. The titration curves at 305 and 340 nm, where the maximum absorption changes occur during the titration, do not show sharp inflection points. This observation is attributed to the stability of the complexes formed between Cu^{2+} and **1TpyT** being lower than that of the complexes formed by Cu^{2+} and **S3**, due in turn to the difference between the steric effects of the ss and ds PNAs on the metal complex.

The titrations of the PNA duplexes **1TpyXC**, which have a central [3 + 1] coordination site, showed clear spectroscopic evidence for the formation of $[Cu(Tpy)_2]^{2+}$ complexes. Specifically, one inflection point was observed in the titration curves at a Cu^{2+}/**1TpyXC** ratio of 1:2 (Figures 5 and S4, Table 2). No further spectroscopic change was observed in the presence of excess Cu^{2+}. Based on these results, we conclude that the formation of interduplex $[Cu(Tpy)_2]^{2+}$ is more favorable than that of $[Cu(Tpy)L]^{2+}$ L = *Py* or *Tz*, although the *Tpy* and L ligands are situated in complementary positions in the duplexes.

The titration curves of the **2TpyY** (Y = C, T) duplexes, which contain a central or terminal pair of *Tpy* ligands, also showed inflection points at Cu^{2+}/**2TpyY** ratio of 1:1, indicative of the formation of $[Cu(Tpy)_2]^{2+}$ complexes. The two *Tpy* ligands in these $[Cu(Tpy)_2]^{2+}$ complexes could originate from the same duplex or could be from different duplexes. A second inflection point was observed for both duplexes at a Cu^{2+}/**2TpyY** ratio of 1:2 (Figures 6, S5, S6), which corresponds to the formation of a $[Cu(Tpy)_2]^{2+}$ complex that must bridge two PNA duplexes (Table 2). This conclusion about the stepwise formation of inter- and intraduplex $[Cu(Tpy)_2]$ complexes is corroborated by the fact that (1) spectral changes observed in the UV spectra of **2TpyY** for Cu^{2+}/**2TpyY** ratios smaller than 1:2 and larger than 1:2 are different, and (2) there is an isosbestic point at 313 nm in the UV spectra of solutions containing Cu^{2+} and **2TpyY** in a ratio Cu^{2+}/**2TpyY** < 1:2 but there is no isosbestic point at 300−320 nm at Cu^{2+}/**2TpyY** ratios between 1:2 and 1:1 (Figures S5a,b and S6a,b).

The logarithm of the apparent stability constants of the $[Cu(Tpy)_2]^{2+}$ and $[Cu(Tpy)]^{2+}$ complexes formed with the free

dx.doi.org/10.1021/ic200855p |*Inorg. Chem.* 2011, 50, 11929–11937

Table 2. Results of UV-vis Titrations of *Tpy* or *Tpy*-PNAs with Cu^{2+}

ligand/PNA	coordination site	isosbestic point (nm)	Cu^{2+}/ dsPNA	Cu^{2+}/ *Tpy*	Logβ' ± SD[a]	Cu^{2+} complex[b]	T_m[c]	handedness[d]
Tpy	free ligand	309		1:2	10.3 ± 0.2	$[Cu(Tpy)_2]^{2+}$		
		319		1:1	4.1 ± 0.2	$[Cu(Tpy)]^{2+}$		
ss S3	central *Tpy*	320	1:2	1:2	10.4 ± 0.3	*inter*-$[Cu(Tpy)_2]^{2+}$		
1TpyT	1 terminal *Tpy*	316	1:2	1:2	9.4 ± 0.5	*inter*-$[Cu(Tpy)_2]^{2+}$	70	left
		320	1:1	1:1	4.6 ± 0.1	$[Cu(Tpy)]^{2+}$		
1TpyPyC	central [*Tpy*−Py]	320	1:2	1:2	9.3 ± 0.1	*inter*-$[Cu(Tpy)_2]^{2+}$	45	left
1TpyTzC	central [*Tpy*−Tz]	320	1:2	1:2	10.3 ± 0.4	*inter*-$[Cu(Tpy)_2]^{2+}$	45	left
2TpyC	central [*Tpy*−*Tpy*]	314	1:2	1:4	10.2 ± 0.4	*inter*-$[Cu(Tpy)_2]^{2+}$	45	right
		331	1:1	1:2	4.0 ± 0.3	*intra*-$[Cu(Tpy)_2]^{2+}$		
2TpyT	terminal [*Tpy*−*Tpy*]	314	1:2	1:4	10.4 ± 0.6	*inter*-$[Cu(Tpy)_2]^{2+}$	70	right
		339	1:1	1:2	4.7 ± 0.2	*intra*-$[Cu(Tpy)_2]^{2+}$		

[a] β' represents the apparent stability constant in 10 mM sodium phosphate buffer at pH 7.0 and 25 °C; SD is the standard deviation. [b] *Inter* and *intra* indicate that the $[Cu(Tpy)_2]^{2+}$ complex is formed between or within PNA duplexes, respectively. [c] Melting temperature measured in the presence of 0.5 equiv of Cu^{2+}/*Tpy*. [d] Handedness of preannealed duplex after addition of Cu^{2+} necessary to form $[Cu(Tpy)_2]$ complex.

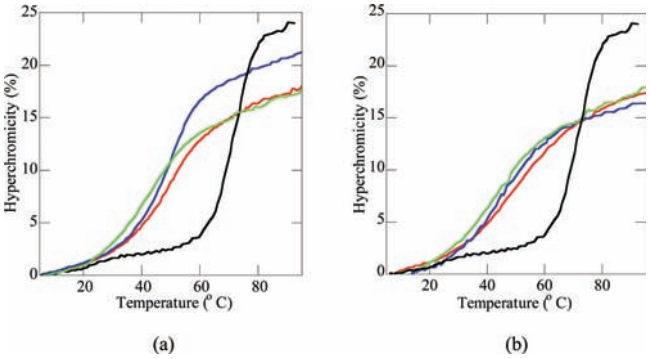

Figure 2. Melting curves of **2TpyC** (red), **1TpyPyC** (blue), and **1TpyTzC** (green) in the absence (a) and presence (b) of 1 equiv of Cu^{2+} per duplex. Solutions were 5 μM dsPNA in 10 mM sodium phosphate buffer at pH 7.0. The melting curve of the nonmodified **PNA** in the absence of Cu^{2+} is also shown (black).

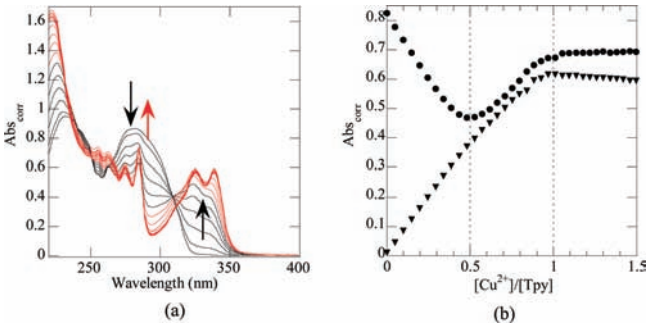

Figure 3. (a) UV−vis spectra for the titration of a 50 μM solution of terpyridine in 10 mM sodium phosphate buffer (pH 7.0) with 500 μM $Cu(NO_3)_2$ aqueous solution, T = 25 °C. Spectra shown in red are for Cu/*Tpy* > 0.5. (b) Titration curves at 286 nm (●) and 340 nm (▼).

ligand or with *Tpy*-modified PNAs were determined from the simulations of the UV spectra. The values for the constants for the complexes formed with the free *Tpy* are 10.3 and 4.1, respectively. The titration curves of **S3**, **1TpyPyC**, and **1TpyPyT** have been simulated assuming the formation of only one type of complex, namely $[Cu(Tpy)_2]^{2+}$. The curves for **1TpyT** have

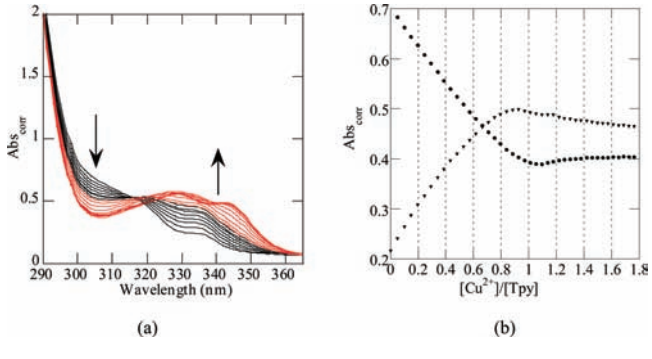

Figure 4. Spectrophotometric titration of a 40 μM solution of duplex **1TpyT** in pH 7.0 10 mM sodium phosphate buffer with 500 μM $Cu(NO_3)_2$ aqueous solution, T = 25 °C. (a) UV−vis spectra for Cu^{2+}/**1TpyT** varying between 0:1 and 1.8:1; (b) titration curves at 305 nm (●) and 340 nm (▼).

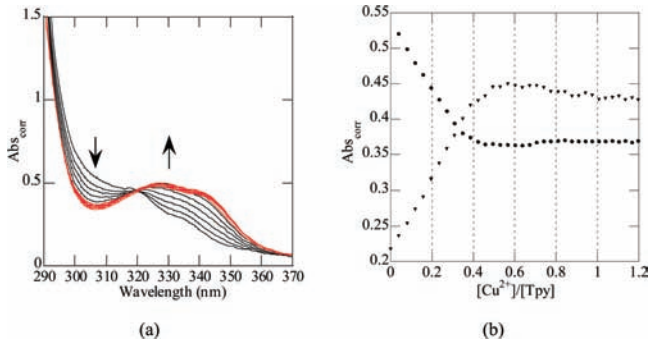

Figure 5. Spectrophotometric titration of a 50 μM solution of duplex **1TpyTzC** in pH 7.010 mM sodium phosphate buffer with 500 μM $Cu(NO_3)_2$ aqueous solution, T = 25 °C. (a) UV−vis spectra for Cu^{2+}/**1TpyTzC** varying between 0:1 and 1.4:1; (b) titration curves at 305 nm (●) and 340 nm (▼).

been simulated assuming the sequential formation of $[Cu(Tpy)_2]^{2+}$ and $[Cu(Tpy)]^{2+}$. It is notable that the stability constants of these complexes are similar to each other and to complexes of Cu^{2+} with the free ligand *Tpy* that have the corresponding stoichiometry.

dx.doi.org/10.1021/ic200855p |*Inorg. Chem.* 2011, 50, 11929–11937

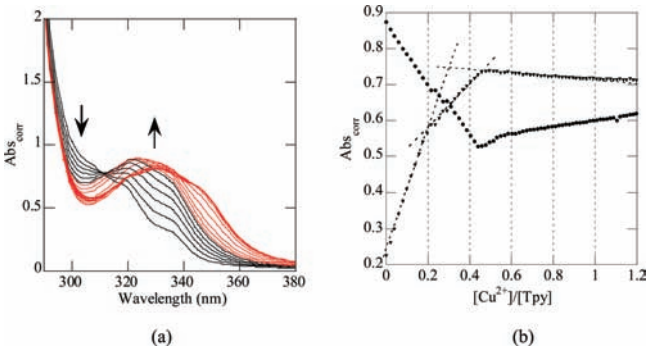

Figure 6. Spectrophotometric titration of a 50 μM solution of duplex **2TpyC** in pH 7.010 mM sodium phosphate buffer with 500 μM $Cu(NO_3)_2$ aqueous solution. (a) UV−vis spectra for Cu^{2+}/ **2TpyC** varying between 0:1 and 1.3:1; (b) titration curves at 305 nm (●) and 340 nm (▼).

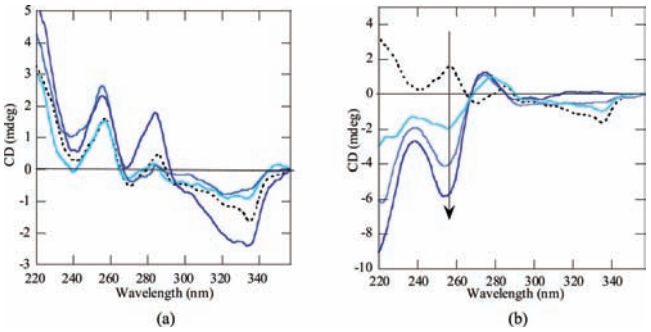

Figure 7. CD spectra of 5 μM of duplex **2TpyT** in 10 mM sodium phosphate buffer at pH 7.0. (a) The duplex was annealed in the absence of Cu^{2+} and then 0.5 (darker blue), 1.0 (darker blue), or 2.0 (darkest blue) equiv of Cu^{2+}/ds**2TpyT** were added to the solution of ds PNA. (b) The duplex was annealed in the presence of 0, 0.5, 1.0, or 2.0 equiv of Cu^{2+}/dsPNA. The dotted black line represents the CD spectrum of the **2TpyT** duplex in the absence of Cu^{2+}.

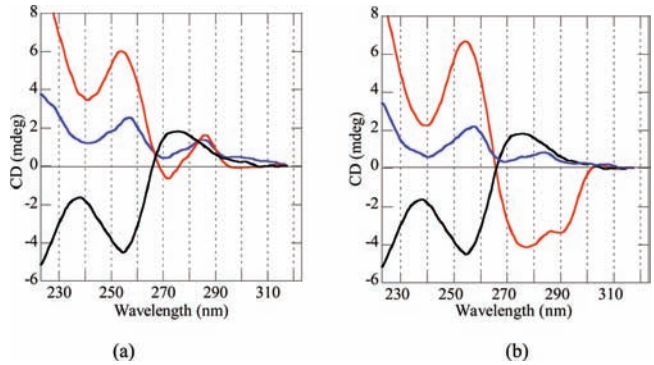

Figure 8. CD spectra of 5 μM solutions of duplexes **2TpyC** (red) and **2TpyT** (blue) in 10 mM sodium phosphate buffer at pH 7.0 annealed in the absence of Cu^{2+} (a), and 1 h after the addition of 1 equiv of Cu^{2+} to the preannealed duplexes (b). For comparison purpose, the CD spectrum of the nonmodified **PNA** in the absence of Cu^{2+} is also shown in black in both panels.

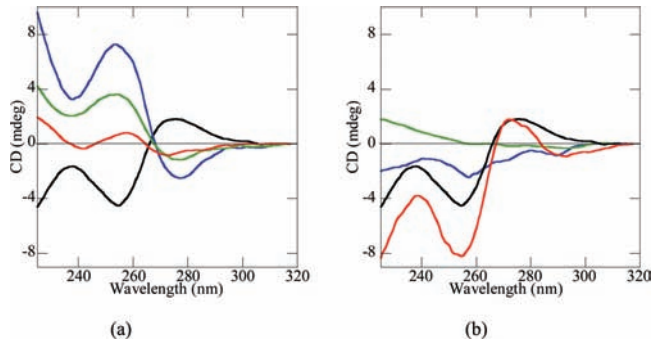

Figure 9. CD spectra of 5 μM solutions of duplexes **1TpyT** (red), **1TpyPyC** (green), and **1TpyTzC** (blue) in 10 mM sodium phosphate buffer at pH 7.0, annealed in the absence of Cu^{2+} (a) and after the addition of 1 equiv of Cu^{2+} to the annealed duplexes (b). For comparison purposes, the CD spectrum of the nonmodified **PNA** in the absence of Cu^{2+} is also shown in black in both panels.

CD Spectroscopy. Single-stranded, Aeg-based PNAs with a C-terminal D-lysine do not show a CD spectrum. Recently, some of us have shown that the incorporation of an (*S*)-Me stereogenic center at the γ-backbone position of a thymine PNA monomer introduced in a ss PNA caused the ss PNA to adopt a right-handed structure.[6b] Interestingly, in the present study we observed that when the same (*S*)-Me stereogenic center was present in the backbone of a *Tpy* monomer, it caused the ssPNA containing the monomer to adopt a left-handed structure (Figure S7). In contrast, the PNA duplexes **1TpyT**, **1TpyPyC**, **1TpyTzC**, **2TpyC**, and **2TpyT** showed a CD spectrum characteristic of a right-handed helix with positive peaks at 220 and 255 nm and a negative peak at 275 nm (Figures 7a, 8a, 9a, S8, S9, and S10). The PNA duplexes that had central (*S*)-*Tpy* monomers had stronger CD features than the duplexes with the same monomer in the terminal position. Based on these CD results, we conclude that the PNA monomer that contains a (*S*)-Me center influences the structure of both ss and ds PNA but that its chiral induction effect is modulated by the nucleobase or ligand with the respective PNA monomer and by the position of the chiral monomer in the PNA.

We have recorded CD spectra of (1) preannealed **2TpyT** duplexes to which 1 equiv of Cu^{2+} per duplex was added (Figure 7a), and (2) **2TpyT** duplexes annealed in the presence of the same amount of Cu^{2+} (Figure 7b). These CD spectra showed that metal binding to the preannealed, right-handed duplex did not change the handedness of the duplex although it caused a change in the structure of the duplex (see changes in the spectral features at 260 and 280 nm in Figure 7a). Notably, the largest change was observed when 0.5 equiv of Cu^{2+} was added to the **2TpyT** duplexes, which corresponds to the existence in solution of dimers of duplexes bridged by inter-$[Cu(Tpy)_2]^{2+}$ complexes. The fact that the handedness of the preannealed duplex is not affected by coordination of Cu^{2+} to *Tpy* means that the Cu^{2+} coordination does not affect the chiral induction effect of the chiral *Tpy*, and suggests that at least one of the two *Tpy* ligands present in each duplex remains in π stacking interactions with the adjacent nucleobases after coordination to Cu^{2+}. In contrast, the PNA duplexes annealed in the presence of Cu^{2+} were left-handed (Figure 7b), which suggests that the handedness of the duplexes formed by annealing in the presence of Cu^{2+} is determined by the terminal L-lysine rather than by the *Tpy*-PNA monomers.

The CD spectra of the preannealed duplex **2TpyC** which Cu^{2+} was added and for duplexes annealed in the presence of Cu^{2+} were identical (Figures 8 and S8). The addition of 1 equiv of Cu^{2+} to the **2TpyC** PNA duplex did not affect the preferred

right-handedness of the duplex, but a new, strong CD feature was observed at 265−300 nm (Figure 8b). This feature was not observed in the CD spectrum of the **2TpyT** duplex to which Cu^{2+} was added, which indicates that the structures of the Cu^{2+}-coordinated **2TpyC** and **2TpyT** duplexes are significantly different.

The CD spectra of duplexes **1TpyT** and **1TpyXC** obtained for preannealed duplexes to which Cu^{2+} was added and for duplexes annealed in the presence of Cu^{2+} were identical (Figures 9 and S9, S10, respectively). Binding of 1 equiv of Cu^{2+} to these duplexes that contain one *Tpy* caused the switch of their handedness from right- to left-handed (Figure 8b). We attribute this observation to the fact that the formation of the intermolecular $[Cu(Tpy)_2]^{2+}$ can cause the *Tpy*s to bulge out of the duplex, and thus prevents the ligand-containing, γ-PNA monomer from exerting a chiral induction effect on the duplex. Consequently, the handedness of the PNA duplexes is determined by the C-terminus, L-lysine, which induces a preference for left-handedness.

Scheme 4. Cartoon Representation of Proposed Structures of Metal-Containing *Tpy*-PNA Duplexes

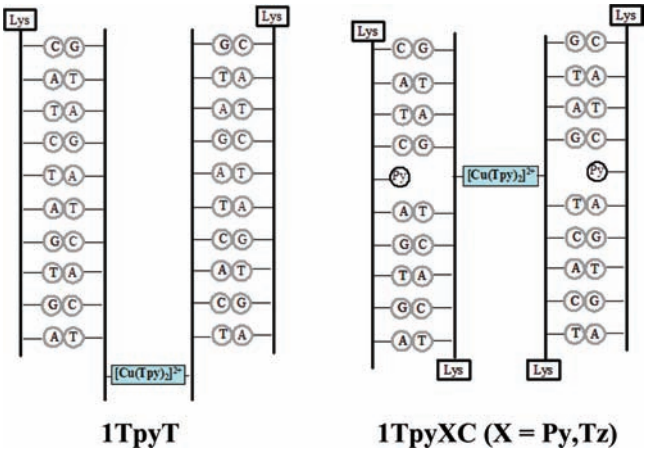

DISCUSSION

Numerous studies have been dedicated in the past decade to the study of nucleic acids in which metal coordination sites have been created by the substitution of nucleobase pairs with pairs of ligands.[2,8] The majority of these sites are designed to be four coordinate and are based on a pair of ligands that are bidentate [2 + 2] or tridentate/monodentate [3 + 1]. The actual coordination number of the metal ion bound to such a site may be higher if the metal co-opts in their coordination sphere one or two solvent molecules or donor atoms from nucleobases that are adjacent to the metal complex. Only a few examples of different coordination types have been purposefully pursued or serendipitously discovered.[9b,25]

In this study, we have incorporated one or two (*S*)-*Tpy* ligands at various positions in PNA duplexes that also contained at least one C-terminal L-Lys. Interestingly, we have observed that the introduction of one central (*S*)-*Tpy* monomer into a ss PNA caused it to adopt a left-handed helical structure. Based on this observation and the previously reported facts that (1) a ss PNA that contained a γ-(*S*) Thymine monomer had a preferred right-handedness,[26] and (2) a ss aeg-PNA with one C-terminal L-Lys does not have a preferred handedness,[3d] we hypothesize that the (*S*)-*Tpy* PNA monomer causes the ss PNA to adopt a structure in which the L-Lys can exert its chiral induction effect but the (*S*)-*Tpy* PNA monomer cannot. NMR studies have indeed shown that short γ-PNAs and γ-PNA duplexes have a backbone more rigid than Aeg-PNA, so it is possible that the (*S*)-*Tpy* ligand favors a rigid secondary structure of the ss PNA in which the L-Lys interacts with adjacent nucleobases but the *Tpy* does not. Interestingly, the duplex formed by the left-handed ss γ-*Tpy* PNA with its complementary strand is right-handed (Figures 8a and 9a), which indicates that the handedness of the duplex is induced by the γ-(*S*)-*Tpy* PNA monomer and not by the L-lysine. To our knowledge, a change in handedness in going from a single-stranded to a double-stranded nucleic acid has not been observed previously. Nevertheless, this effect is reminiscent of the change in local handedness observed in a PNA oligomer by Petersson et al.[3b] In their studies, crystallization of a partly self-complementary, single-stranded PNA led to a structure that included duplex and triplex sections with different handedness. The switch in handedness meant that backbone configurations of opposite handedness existed in the same PNA oligomer. Furthermore, we have observed in the crystal structure of a *Bipy*-modified PNA duplex that it is possible for a central PNA monomer to bulge out of the duplex without perturbing the regular P-type helix adopted by the rest of the nucleobase pairs flanking the respective monomer, a position that could be also adopted by the (*S*)-Me *Tpy* monomer in the PNA duplexes.

The CD features of the **2TpyC** duplex are more intense than those of the **2TpyT** duplex, indicating that the pair of γ-*Tpy* ligands has a stronger chiral induction effect when situated in the center rather than at the end of the duplex. This observation makes sense given that (1) previous studies of the chiral effect of terminal amino acids on a PNA duplex showed that an N-terminal L-lysine exerts a weaker chiral induction effect than a C-terminal L-lysine,[26] and (2) one of the γ-*Tpy* monomers of the duplex **2TpyT** is at the N-terminus of a strand. The handedness of the preannealed **2TpyY**, Y= C, T, duplexes was not changed upon Cu^{2+} addition, which indicates that the metal complex does not change the relative orientation of at least one of the *Tpy* ligands with respect to the duplex and that the respective chiral ligand exerts its chiral induction effect in the duplex. We note that the CD spectra of several PNA duplexes, namely **1TpyT**, **1TpyTzC**, **2TpyC**, and **2TpyT** have small features at 280−300 nm, which may be due to *Tpy* because the ligand has an absorption band in this spectral range (Figure 3).

We discovered that irrespective of the number and position of the *Tpy* ligands in the PNA duplex, the addition of 0.5 equiv of Cu^{2+} per *Tpy* ligand leads to $[Cu(Tpy)_2]^{2+}$ complexes with [3 + 3] coordination. We conclude that the high stability constant of the complex ($\log K$ = 19.1)[27] favors its formation even if a tetrazole or pyridine are situated across the *Tpy* and a [3 + 1] complex could be formed within the PNA duplex. Steric interactions may also disfavor the formation of a [3 + 1] complex within the duplex. In the case of the **1TpyXC** complexes, the [3 + 3] $[Cu(Tpy)_2]^{2+}$ complex must bridge a pair of PNA duplexes and the *Tpy* ligands must be bulged out of each duplex (Scheme 4). This geometric relationship between the metal complex and duplex is corroborated by the fact that there is a slight decrease in the T_m of the duplexes in the presence of Cu^{2+}, as expected if the intermolecular $[Cu(Tpy)_2]^{2+}$ complex poses a steric challenge to the duplex. Furthermore, the switch in the preferred handedness of these duplexes upon addition of Cu^{2+}

dx.doi.org/10.1021/ic200855p |*Inorg. Chem.* 2011, 50, 11929–11937

can be rationalized if the metal coordination causes the *S-Tpy* PNA monomer to bulge out of the duplex, perturbs its $\pi-\pi$ stacking with neighboring base pairs, and hinders the transmission of the chiral induction effect of (*S*)-*Tpy*. In other words, the dominant effect exerted by the *Tpy* ligand in the absence of Cu^{2+} on the right-handedness of the duplex cannot manifest upon the bulging out of the *Tpy* to coordinate to Cu^{2+}, and hence the C-terminal L-Lys determines the preferred left-handedness of the duplex. We note that the conclusion that a [3 + 1] metal complex is not formed within the **1TpyXC** duplexes does not rule out the possibility that such a complex could be formed in duplexes with a different sequence, with a different monodentate ligand, or if the ligands are differently attached to the PNA backbone. This is because we have shown that the sequence of the duplex and the way in which a ligand is attached to the PNA backbone influence the stability constant of metal complexes formed within nucleic acid duplexes.[28]

The addition of 1 equiv of Cu^{2+} to duplexes **2TpyY**, which have a pair of central or terminal *Tpy*s led as expected to the formation of one $[Cu(Tpy)_2]^{2+}$ complex per PNA duplex. The two *Tpy* ligands of the $[Cu(Tpy)_2]^{2+}$ complex cannot be coplanar, which means that it is not possible for the complex to "fit" in the place of one planar nucleobase pair. Consequently, steric interactions between the complex and the adjacent nucleobases are likely to destabilize the duplex. This effect can explain why the melting temperature of **2TpyY** duplexes is the same in the presence and absence of the Cu^{2+} although one would have expected that the coordinative bonds between Cu^{2+} and the *Tpy* ligands stabilize the duplex and increase its melting temperature. Instead, the destabilization effect of steric interactions diminishes the stabilization of the duplex by coordination bonds that are stronger than hydrogen bonds.

Interestingly, the UV−vis titrations of the **2TpyC** and **2TpyT** duplexes showed that a complex forms between Cu^{2+} and *Tpy* not only at a Cu^{2+}/ds *Tpy*-PNA ratio of 1:1 but also at a ratio of 1:2, which corresponds to a Cu^{2+}/*Tpy* ratio of 1:4. As attainment of a coordination number higher than six for Cu^{2+} or the accommodation around Cu^{2+} of four *Tpy* ligands originating from a minimum of two PNA duplexes are extremely unlikely, our hypothesis is that upon addition of 0.5 equiv of Cu^{2+}/**2TpyY** PNA duplex, an interduplex $[Cu(Tpy)_2]^{2+}$ complex forms and bridges the two **2TpyY** duplexes. The CD spectra of the two duplexes in the presence of 0.5 equiv of Cu^{2+} can be understood based on this hypothesis; specifically, the handedness of the duplex is not affected by the formation of the interduplex $[Cu(Tpy)_2]^{2+}$ complex, which is extrinsic to the duplex, although its structure is affected by steric interactions between the bulged out complex and the duplex.

The existence of intermolecular $[M(Tpy)_2]$ complexes that bridge nucleic acid oligomers and duplexes has been previously reported. For example, DNA triangles with edges made of DNA duplexes and corners of $[Fe(Tpy)_2]^{2+}$ complexes have been assembled in the presence of Fe^{2+} from DNA oligomers that had a terminal *Tpy* ligand.[12a] In another example, Fe^{2+} coordination to a DNA single strand with a terminal *Tpy* caused the formation of a $[Fe(Tpy)_2]$ complex with two appended single stranded DNAs.[12b] To our knowledge, in almost all nucleic acid-based structures connected by $[M(Tpy)_2]$ complexes, the *Tpy* ligand was attached to the end of the DNA strands.[12,29] In a very recent example, Burns et al. incorporated *Tpy* ligands away from the ends of DNA duplexes and used the ligands to create an extended network of duplexes.[30] These studies show that, as one would expect, the bridging of nucleic acids by coordination complexes with ligands from different single- or double-strand nucleic acids is not a property specific to PNA but a general one that can be used to synthesize extended, nucleic acid-based nanostructures.

The effect of Cu^{2+} on the structure and handedness of the **2TpyT** was different depending on whether Cu^{2+} was present during the annealing of the duplex or was added after the duplex was annealed. When annealed in the absence of Cu^{2+}, the duplex adopted a right-handed structure, which must be determined by the *S-Tpy* ligand. The CD spectra showed that the Cu^{2+} coordination to the *Tpy* ligands of the preannealed duplex affects the structure of the duplex but not its handedness. In contrast, when the duplex was annealed in the presence of Cu^{2+} ions, it adopted a left-handed structure. This difference must be related to the fact that at high temperature and in the presence of Cu^{2+}, the *Tpy*-containing ss PNA can form the $[Cu(Tpy)_2]^{2+}$ complex, which prevents the nucleobase pairs adjacent to the complex from interacting with each other and with the complex in the same way in which they do in the preannealed duplex. Hence the chiral induction effect of (*S*)-*Tpy* cannot manifest and the handedness of the duplex is induced by the C-terminal L-lysine.

CONCLUSIONS

Investigations carried out on five duplexes that contained one or two γ-modified *Tpy* PNA monomers have shown that in the presence of Cu^{2+} these duplexes form a $[Cu(Tpy)_2]^{2+}$ complex irrespective of the number and position of the *Tpy* ligands in the duplex because the complex is very stable. This property precluded the formation of [3 + 1] alternative base pairs in the duplexes that contained a monodentate ligand in the position complementary to the tridentate *Tpy* ligand, but made possible the synthesis of dimers of PNA duplexes bridged by a $[Cu(Tpy)_2]^{2+}$ complex. We have also found that a γ-Me *Tpy* PNA monomer exerts a chiral induction effect on single-stranded PNA when introduced at another position than the N-terminus of the strand. This effect was altered by the Watson Crick hybridization of PNA strands into duplexes and by Cu^{2+} coordination to *Tpy*. These observations are of value for the design of hybrid inorganic−nucleic acid structures with specific structural properties.

ASSOCIATED CONTENT

Supporting Information. Description of the synthesis of terpyridine PNA monomers, UV melting curves, UV titrations and CD spectra of *Tpy* PNA in the absence and presence of Cu^{2+}. This material is available free of charge via the Internet at http://pubs.acs.org.

AUTHOR INFORMATION

Corresponding Author

*E-mail: achim@cmu.edu. Phone: 412 268 9588. Fax: 412 268 1061.

ACKNOWLEDGMENT

We thank the U.S. National Science Foundation for support of this work (CHE-0848725). The Center for Molecular Analysis and the NMR Facility at Carnegie Mellon are supported in part by NSF (CHE-9808188, 0130903, and 1039870).

REFERENCES

(1) Clever, G. H.; Shionoya, M. *Coord. Chem. Rev.* **2011**, *254*, 2391–2402.

(2) He, W.; Franzini, R. M.; Achim, C. *Prog. Inorg. Chem.* **2007**, *55*, 545–611.

(3) (a) He, W.; Hatcher, E.; Balaeff, A.; Beratan, D.; Gil, R. R.; Madrid, M.; Achim, C. *J. Am. Chem. Soc.* **2008**, *130*, 13264–13273. (b) Petersson, B.; Nielsen, B. B.; Rasmussen, H.; Larsen, I. K.; Gajhede, M.; Nielsen, P. E.; Kastrup, J. S. *J. Am. Chem. Soc.* **2005**, *127*, 1424–1430. (c) Rasmussen, H.; Kastrup, J. S.; Nielsen, J. N.; Nielsen, J. M.; Nielsen, P. E. *Nat. Struct. Biol.* **1997**, *4*, 98–101. (d) Rasmussen, H.; Liljefors, T.; Petersson, B.; Nielsen, P. E.; Kastrup, J. S. *J. Biomol. Struct. Dyn.* **2004**, *21*, 495–502. (e) Yeh, J. I.; Pohl, E.; Truan, D.; He, W.; Sheldrick, G. M.; Du, S.; Achim, C. *Chem.—Eur. J.* **2010**, *16*, 11867–11875.

(4) (a) Brasun, J.; Ciapetti, P.; Kozlowski, H.; Oldziej, S.; Taddei, M.; Valensin, D.; Valensin, G.; Gaggelli, N. *Dalton Trans.* **2000**, 2639–2644. (b) Lagriffoule, P.; Wittung, P.; Eriksson, M.; Jensen, K. K.; Norden, B.; Buchardt, O.; Nielsen, P. E. *Chem.—Eur. J.* **1997**, *3*, 912–919. (c) Totsingan, F.; Jain, V.; Bracken, W. C.; Faccini, A.; Tedeschi, T.; Marchelli, R.; Corradini, R.; Kallenbach, N. R.; Green, M. M. *Macromolecules* **2010**, *43*, 2692–2703. (d) Wittung, P.; Eriksson, M.; Lyng, R.; Nielsen, P. E.; Norden, B. *J. Am. Chem. Soc.* **1995**, *117*, 10167–73.

(5) (a) Sforza, S.; Haaima, G.; Marchelli, R.; Nielsen, P. E. *Eur. J. Org. Chem.* **1999**, 197–204. (b) Sforza, S.; Tedeschi, T.; Corradini, R.; Marchelli, R. *Eur. J. Org. Chem.* **2007**, 5879–5885.

(6) (a) Pensato, S.; Saviano, M.; Bianchi, N.; Borgatti, M.; Fabbri, E.; Gambari, R.; Romanelli, A. *Bioorg. Chem.* **2010**, *38*, 196–201. (b) Rapireddy, S.; He, G.; Roy, S.; Armitage, B. A.; Ly, D. H. *J. Am. Chem. Soc.* **2007**, *129*, 15596–15600.

(7) Atwell, S.; Meggers, E.; Spraggon, G.; Schultz, P. G. *J. Am. Chem. Soc.* **2001**, *123*, 12364–12367.

(8) Clever, G. H.; Kaul, C.; Carell, T. *Angew. Chem., Int. Ed.* **2007**, *46*, 6226–6236.

(9) (a) Watson, R. M.; Skorik, Y. A.; Patra, G. K.; Achim, C. *J. Am. Chem. Soc.* **2005**, *127*, 14628–39. (b) Franzini, R. M.; Watson, R. M.; Patra, G. K.; Breece, R. M.; Tierney, D. L.; Hendrich, M. P.; Achim, C. *Inorg. Chem.* **2006**, *45*, 9798–9811. (c) Popescu, D.-L.; Parolin, T. J.; Achim, C. *J. Am. Chem. Soc.* **2003**, *125*, 6354–6355.

(10) Mueller, J.; Freisinger, E.; Lax, P.; Megger, D. A.; Polonius, F.-A. *Inorg. Chim. Acta* **2007**, *360*, 255–263.

(11) Heuberger, B. D.; Shin, D.; Switzer, C. *Org. Lett.* **2008**, *10*, 1091–1094.

(12) (a) Choi, J. S.; Kang, C. W.; Jung, K.; Yang, J. W.; Kim, Y.-G.; Han, H. *J. Am. Chem. Soc.* **2004**, *126*, 8606–8607. (b) Goeritz, M.; Kraemer, R. *J. Am. Chem. Soc.* **2005**, *127*, 18016–18017. (c) Lin, C.; Liu, Y.; Yan, H. *Biochemistry* **2009**, *48*, 1663–1674.

(13) (a) Chenna, V.; Rapireddy, S.; Sahu, B.; Ausin, C.; Pedroso, E.; Ly, D. H. *ChemBioChem* **2008**, *9*, 2388–2391. (b) Koch, T. *Pept. Nucleic Acids (2nd Ed.)* **2004**, 37–59.

(14) (a) Wolpher, H.; Sinha, S.; Pan, J.; Johansson, A.; Lundqvist, M. J.; Persson, P.; Lomoth, R.; Bergquist, J.; Sun, L.; Sundstroem, V.; Akermark, B.; Polivka, T. *Inorg. Chem.* **2007**, *46*, 638–651. (b) Armspach, D.; Constable, E. C.; Diederich, F.; Housecroft, C. E.; Nierengarten, J.-F. *Chem.—Eur. J.* **1998**, *4*, 723–733.

(15) Christensen, L.; Fitzpatrick, R.; Gildea, B.; Petersen, K. H.; Hansen, H. F.; Koch, T.; Egholm, M.; Buchardt, O.; Nielsen, P. E.; Coull, J.; et al. *J. Pept. Sci.* **1995**, *1*, 175–83.

(16) Dueholm, K. L.; Egholm, M.; Behrens, C.; Christensen, L.; Hansen, H. F.; Vulpius, T.; Petersen, K. H.; Berg, R. H.; Nielsen, P. E.; Buchardt, O. *J. Org. Chem.* **1994**, *59*, 5767–73.

(17) NIST Chemistry WebBook. http://webbook.nist.gov.

(18) Gans, P.; Sabatini, A.; Vacca, A. *Talanta* **1996**, *43*, 1739–1753.

(19) Ohr, K.; Gilmartin, B. P.; Williams, M. E. *Inorg. Chem.* **2005**, *44*, 7876–7885.

(20) Coppock, M. B.; Kapelewski, M. T.; Youm, H. W.; Levine, L. A.; Miller, J. R.; Myers, C. P.; Williams, M. E. *Inorg. Chem.* **2010**, *49*, 5126–5133.

(21) Coppock, M. B.; Miller, J. R.; Williams, M. E. *Inorg. Chem.* **2011**, *50*, 949–955.

(22) (a) Wittung, P.; Nielsen, P. E.; Buchardt, O.; Egholm, M.; Norden, B. *Nature* **1994**, *368*, 561–3. (b) Egholm, M.; Buchardt, O.; Christensen, L.; Behrens, C.; Freier, S. M.; Driver, D. A.; Berg, R. H.; Kim, S. K.; Norden, B.; Nielsen, P. E. *Nature* **1993**, *365*, 566–8.

(23) Datta, B.; Armitage, B. A. *J. Am. Chem. Soc.* **2001**, *123*, 9612–9619.

(24) Dobrawa, R.; Lysetska, M.; Ballester, P.; Gruene, M.; Wuerthner, F. *Macromolecules* **2005**, *38*, 1315–1325.

(25) (a) Takezawa, Y.; Tanaka, K.; Yori, M.; Tashiro, S.; Shiro, M.; Shionoya, M. *J. Org. Chem.* **2008**, *73*, 6092–6098. (b) Tanaka, K.; Yamada, Y.; Shionoya, M. *J. Am. Chem. Soc.* **2002**, *124*, 8802–8803. (c) Zimmermann, N.; Meggers, E.; Schultz, P. G. *J. Am. Chem. Soc.* **2002**, *124*, 13684–13685.

(26) Dragulescu-Andrasi, A.; Rapireddy, S.; Frezza, B. M.; Gayathri, C.; Gil, R. R.; Ly, D. H. *J. Am. Chem. Soc.* **2006**, *128*, 10258–10267.

(27) Martell, A. E.; Smith, R. M. *Critical Stability Constants*; Plenum Press: New York, 1976, Vol. 4; 495 pp.

(28) Ma, Z.; Olechnowicz, F.; Skorik, Y. A.; Achim, C. *Inorg. Chem.* **2011**, *50*, 6083–6092.

(29) Ghosh, S.; Pignot-Paintrand, I.; Dumy, P.; Defrancq, E. *Org. Biomol. Chem.* **2009**, *7*, 2729–2737.

(30) Burns, J. R.; Zekonyte, J.; Siligardi, G.; Hussain, R.; Stulz, E. *Molecules* **2011**, *16*, 4912–4922.